Two Rate-Limiting Steps in the Kinetic Mechanism of the Serine/Threonine Specific Protein Kinase ERK2: A Case of Fast Phosphorylation Followed by Fast Product Release†

William F. Waas,‡,§ Mark A. Rainey,|| Anna E. Szafranska,‡ and Kevin N. Dalby*,‡,§,||,⊥

Division of Medicinal Chemistry, College of Pharmacy, and Graduate Programs in Pharmacy, Biochemistry, and Molecular Biology, University of Texas at Austin, Austin, Texas 78712

Received May 22, 2003; Revised Manuscript Received August 14, 2003

ABSTRACT: Extracellular regulated protein kinase 2 (ERK2) is a eukaryotic protein kinase whose activity is regulated by mitogenic stimuli. To gain insight into the catalytic properties of ERK2 and to complement structure−function studies, we undertook a pre-steady state kinetic analysis of the enzyme. To do this, ERK2 was quantitatively activated by MAPKK1 *in vitro* by monitoring the stoichiometry and site specificity of phosphorylation using a combination of protein mass spectrometry, tryptic peptide analysis, and ^{32}P radiolabeling. Using a quench-flow apparatus, $MgATP^{2-}$ was rapidly mixed (<1 ms) with both ERK2 and the protein substrate EtsΔ138 in the presence of a saturating total concentration (20 mM) of magnesium ion at 27 °C and pH 7.5. An exponential burst of product was observed over the first few milliseconds that followed mixing. This burst had an amplitude α of 0.44 and was followed by a slower linear phase. The pre-steady state burst is consistent with two partially rate-limiting enzymatic steps, which have the following rate constants: $k_2 = 109 \pm 9\ s^{-1}$ and $k_3 = 56 \pm 4\ s^{-1}$. These are attributed to rapid phosphorylation of EtsΔ138 and the process of product release, respectively. Single-turnover experiments provided an independent determination of k_2 ($106 \pm 25\ s^{-1}$). The observed catalytic constant (k_{cat}^{obs}) was found to be sensitive to the concentration of ERK2. The data fit a model in which ERK2 monomers form dimers and suggest that both the monomeric and dimeric forms of ERK2 are active with catalytic constants (k_{cat}) of 25 and 37 s^{-1}, respectively. In addition, the model suggests that in the presence of saturating concentrations of both magnesium and substrates ERK2 subunits dissociate with a dissociation constant (K_d) of 32 ± 16 nM.

We are interested in the mechanism and regulation of the extracellular regulated protein kinases (ERK1[1] and ERK2) because of their key roles in cellular signal transduction and disease (*5*−*7*). Both enzymes are activated through a protein kinase cascade, termed the mitogen-activated protein kinase cascade, which is activated by mitogenic stimuli (*8*, *9*). A common mediator is Ras, a small guanine nucleotide binding protein that transduces extracellular signals to the cell nucleus (*10*). This pathway is a current focus in the biomedical community because of a number of links between its deregulation and cancer (*11*).

ERK2 catalyzes the transfer of the γ-phosphate of adenosine triphosphate to serine or threonine residues found in Ser-Pro or Thr-Pro motifs on proteins (*12*). The basis for the proline specificity of ERK2 is not clear, and in fact, the mechanism by which it interacts with substrates is not well understood. Like those of several other serine/threonine specific protein kinases, interactions extraneous to the active site appear to be critical determinants of specificity, which is not surprising given the preponderance of Ser/Thr-Pro motifs found on the surfaces of cellular proteins (*13*, *14*). Mutagenesis studies on a number of substrates have been useful in identifying discrete linear sequences termed docking domains that mediate interactions with their cognate MAPKs, but are situated some distance, typically more than 50 amino acids, from the phosphorylation sites (*15*−*23*). In addition, the sequence FXF appears to be a specificity determinant for ERK2 that resides somewhat closer to the phosphorylation sites than the docking domains (*24*). Substrate binding

† This research was supported in part by the Welch Foundation (Grant F-1390), the National Institutes of Health (Grant GM59802), and Analytical Instrumentation Facility Core Grant P30 ES07784. W.F.W. was a recipient of a National Research Service Award, NIH Biotechnology Predoctoral Training Grant T32 GM08474.

* To whom correspondence should be addressed: Division of Medicinal Chemistry, College of Pharmacy, University of Texas at Austin, Austin, TX 78712. Telephone: (512) 471-9267. Fax: (512) 232-2606. E-mail: Dalby@mail.utexas.edu.

‡ Division of Medicinal Chemistry, College of Pharmacy.

§ Graduate Program in Pharmacy.

|| Graduate Program in Molecular Biology.

⊥ Graduate Program in Biochemistry.

[1] Abbreviations: MAPKK, MAP kinase kinase; ERK, extracellular regulated protein kinase; MAPK, mitogen-activated protein kinase; MALDI, matrix-assisted laser desorption ionization; MKK1G7B, constitutively active recombinant human mitogen-activated protein kinase kinase 1 (ΔN4/S218D/M219D/N221D/S222D), where ΔN4 indicates a deletion of residues 32−43; EtsΔ138, polyhistidine-tagged Ets-1(1−138); EtsΔ138∼P, polyhistidine-tagged Ets-1(1−138) phosphorylated on Thr-38; EDTA, ethylenediaminetriacetic acid; EGTA, ethylene glycol bis(β-aminoethyl ether)-*N*,*N*,*N*′,*N*′-tetraacetic acid; DEAE, diethylaminoethyl; DTT, dithiothreitol; HEPES, 4-(2-hydroxyethyl)-1-piperazineethanesulfonic acid; PMSF, phenylmethanesulfonyl fluoride; Tris, tris(hydroxymethyl)aminomethane; TFA, trifluoroacetic acid; BSA, bovine serum albumin; BMN, benzylidene malononitrile; PCR, polymerase chain reaction; LC−MS, liquid chromatography−mass spectrometry.

10.1021/bi0348617 CCC: $25.00
Published on Web 09/30/2003

sites have also been subjected to investigation, where, for example, mutagenesis studies on p38 MAPKα and ERK2, together with two X-ray crystal structures of peptides complexed to p38 MAPK, point to two shallow grooves and a charged region termed the CD domain as possible substrate binding sites (*25*−*29*).

However, despite some considerable effort many questions remain. For example, the kinetic and thermodynamic contributions of specific amino acids to binding and turnover remain to be elaborated. Currently, it is not possible to identify a substrate "docking" sequence on the basis of sequence information alone, and in many cases, such as transcription factor c-Myc, a docking sequence has not been identified. Progress in understanding the energetics of the MAPK enzymes requires a combined kinetic and structural approach, which we initiated some time ago. Initially, we reported kinetic evidence for a random-order ternary complex mechanism for the phosphorylation of transcription factor Ets-1 by ERK2 (*4*). This study was significant because it established that a protein substrate could be used to provide high-quality kinetic data for this enzyme. The substrate used in this study was EtsΔ138, a model protein substrate derived from the N-terminus of Ets-1, which is currently the most thoroughly characterized protein substrate of ERK2. Mutation of Phe-120 in EtsΔ138 to alanine decreases the specificity of ERK2 toward EtsΔ138 some 20−40-fold, suggesting that this residue could be an important ERK2 docking site (*22*). Interestingly, Phe-120 lies in a globular portion of the substrate, in stark contrast to Thr-38, the phosphorylation site, which lies in an extended disordered region of Ets-1 near the N-terminus (*30*) (Figure 1). On the basis of this structure, it is predicted that a significant portion of EtsΔ138 will become ordered upon binding ERK2.

The phosphorylation of Tyr-183 and Thr-185 leads to considerable catalytic activation of ERK2. While activation results in a large (>10000-fold) increase in the specificity constant k_{cat}, it is also be accompanied by slight decreases in the Michaelis parameters (*31*−*34*).[2] Surprisingly, the rate-limiting step for the phosphorylation of myelin basic protein by ERK2 is reported to be phosphoryl transfer (*3*), which is uncommon for protein kinases. In addition, efficient turnover of EtsΔ138 by ERK2 requires activation by Mg^{2+} ions (*1*). Currently, ERK2 is the only serine/threonine specific protein kinase known to be activated by magnesium, although several tyrosine kinases display a similar dependence[3] and preliminary work suggests that this might be the case for other MAPKs also (W. F. Waas and K. N. Dalby, unpublished observations).

We set out to examine the catalytic mechanism of ERK2 with the view that a better understanding of its catalytic strategy will aid the design of potent inhibitors. Protein kinases catalyze the phosphoryl transfer reaction between ATP and a hydroxyl acceptor (R-OH) to form a phosphate monoester of serine, threonine, or tyrosine, a stable but enzymatically reversible modification that invariably regulates a protein's cellular function. The protein kinase family, which is comprised of some 500 members, displays a conserved catalytic domain, embedded between divergent and often regulatory N- and C-termini (*35*). Despite their importance, the basis for their catalytic efficiency is still not well understood. In general, model studies of phosphoryl transfer exhibit a concerted mechanism, through a single transition state, with both the nucleophile and the leaving group undergoing simultaneous covalency change [termed a D_NA_N mechanism (*36*)]. Typically, these reactions are dissociative in nature with only minimal bonding of either the nucleophile or the leaving group to the central phosphorus at the transition state.[4] While there is a suggestion that models can display characteristics of an associative mechanism (*37*), so far there is no firm evidence to support such a mechanism on an enzyme. Indeed, the long axial P−O bond lengths reported in two recently determined X-ray crystal structures appear to provide evidence of enzyme-bound metaphosphate ions (*38*, *39*).

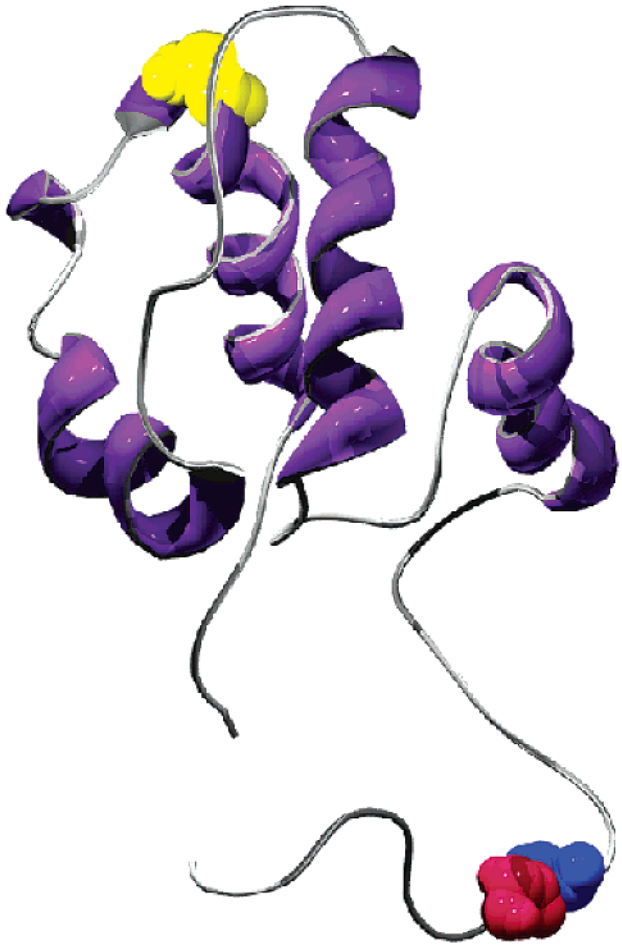

FIGURE 1: Three-dimensional structure of residues 29−138 of Ets-1. Thr-38 is shown in red, Pro-39 in blue, and Phe-120 in yellow. Taken from PDB entry 1BQV (*30*).

[2] Kinetic terms: k_{cat}^{obs}, observed specificity constant; k_{cat}^{D}, specificity constant of each active site in an ERK2 dimer; k_{cat}^{M}, specificity constant of each active site in an ERK2 monomer; k_b, burst rate constant; α, burst amplitude; v_{ss}, steady state velocity; K_d, dissociation constant of ERK2 subunits in the presence of saturating substrates, according to Scheme 2; k_p, rate constant for phosphoryl transfer; E_0, concentration of total ERK2; E_M, concentration of monomeric ERK2; E_D, concentration of dimeric ERK2; *t**, dead time of the rapid quench apparatus; K_{iC}^{app}, apparent competitive inhibition constant.

[3] See Table 4 in ref *1*.

[4] A dissociative transition state is defined as a state where there is less than 50% bond formation between the nucleophile and the phosphorus occurring before the leaving group−phosphorus bond is at least 50% broken (*2*).

Our initial goal was to delineate the reaction pathway for ERK2. To reach this goal, we used the N-terminus of transcription factor Ets-1, EtsΔ138, as our model protein substrate (*40*), which has proven to be an extremely useful substrate for mechanistic studies of ERK2 (*1*, *4*). Although a steady state viscosity approach has been used by others to elucidate the reaction pathway of ERK2 (*32*) and other protein kinases (*41*−*47*), it is not without limitations, and even with the appropriate controls for solvent effects (*48*), it is not always easy to evaluate. In the case presented here, what appeared to be insurmountable solvent effects ruled out the approach. Therefore, a pre-steady state rapid quench approach, which has been used on a number of protein kinases, was used (*49*−*53*). This approach can establish the kinetic pathway directly and identify the rate-limiting step(s) in the overall pathway. In addition, this approach provides for the observation of reactions at the active site of the enzyme such as transiently formed intermediates and changes in protein conformation. Importantly, it can also lay the foundation for detailed structure−function studies.

We report a rapid quench analysis of ERK2 at concentrations of ERK2 that are physiologically relevant. We show that the reaction pathway for the turnover of transcription factor EtsΔ138 occurs through two partially rate-limiting steps. One step correlates with phosphorylation of EtsΔ138 on the enzyme, while the second step is related to product release. In contrast to a previous report, where the general kinase substrate myelin basic protein was used as the substrate (*3*), phosphorylation occurs at a rate 3-fold faster than the steady state rate. In addition, in the Appendix we provide evidence of kinetically significant dimerization of "activated" ERK2, a process first noted by Khokhlatchev *et al*. (*54*). The analysis presented here is notable, because ERK2 is efficiently activated by post-translational phosphorylation in the laboratory where it is minimally 95% active and thus ideal for transient kinetic studies. Furthermore, it should be emphasized that a mechanistic investigation of a protein kinase using a protein substrate provides the experimental basis for critically examining fundamental questions of the enzyme that cannot be answered with peptide substrates. An excellent example of how an enzyme's true colors are only revealed when a *bona fide* substrate is used was reported recently by Park and Raines (*55*).

MATERIALS AND METHODS

Buffers, Proteins, and Reagents. Trizma base was from EM Industries (Gibbstown, NJ). Sigma (St. Louis, MO) provided all other buffer components and chemicals. Qiagen Inc. (Valencia, CA) supplied Ni−NTA agarose and the QIAprep Spin Miniprep kit. Kinase assays were conducted with Roche (Indianapolis, IN) special quality sodium adenosine triphosphate ($Na_2^+ATPH_2^{2-}$) and [γ-^{32}P]$(NH_4^+)_4$-ATP^{4-} from ICN (Costa Mesa, CA). Plasmids used to express (His_6-tagged) ERK2 (*56*) and (His_6-tagged) Ets-1-(1−138) (*30*) have been reported previously. Stock solutions of $Na_2^+ATPH_2^{2-}$ were titrated to pH 8.0 with 1 M potassium hydroxide. All concentrations were determined spectrophotometrically at 259 nm, assuming an extinction coefficient ϵ of 15 400 cm^{-1} M^{-1}. The amount of hydrolyzable ATP^{4-} was determined using a hexokinase−glucose-6-phosphate dehydrogenase coupled assay (*57*). Spectral changes during coupled assays ($NADH-NAD^+$) were monitored at 340 nM using an extinction coefficient ϵ of 6300 cm^{-1} M^{-1} to calculate adenosine triphosphate concentrations. Comparison of the two methods gave values that differed by less than 2%. Tryptone, yeast extract, and agar were obtained from US Biological (Swampscott, MA), Fluka (St. Louis, MO), and BD (Sparks, MD). The thin-walled PCR tubes were obtained from Ambion, Inc. (Austin, TX). Restriction enzymes, PCR reagents, and T4 DNA ligase were obtained from F. Hoffmann-La Roche, Ltd. (Basel, Switzerland), Promega Corp. (Madison, WI), or New England Biolabs (Beverly, MA). The remaining molecular biology reagents, including agarose, DNA ladders, and protein molecular mass standards, were obtained from Invitrogen Corp. (Carlsbad, CA). Oligonucleotides for DNA amplification and sequencing were synthesized by Genosys (The Woodlands, TX).

Strains. Escherichia coli strain DH5α (Invitrogen) was used for cloning and isolation of plasmids. *E. coli* strain BL21(DE3) pLysS from Novagen (Madison, WI) was used for recombinant protein expression.

General Methods. Techniques for restriction enzyme digestion, ligation, transformation, and other standard molecular biology manipulations were based on methods described by the manufacturer. Plasmid DNA was introduced into cells by electroporation using a BTX Transporter Plus. The PCR was performed on a Techno DNA thermal cycler. DNA sequencing was done at the DNA Core Facility in the Institute for Cellular and Molecular Biology at the University of Texas at Austin. UV−visible spectra were obtained on a CARY 50 Varian UV spectrophotometer. FPLC was performed on a Pharmacia ÄKTA FPLC or Waters FPLC system using a Mono Q HR 10/10 column. HPLC was performed on a Waters HPLC system using a 250 mm × 4 mm Vydac RP C_{18} column (218TP54). Protein was analyzed by Tris glycine sodium dodecyl sulfate−polyacrylamide gel electrophoresis (SDS−PAGE) under denaturing conditions on 10 to 15% gels using the Mini-Protean III vertical gel electrophoresis apparatus obtained from Bio-Rad (Hercules, CA).

Preparation and Purification of Proteins. (1) (His_6-Tagged) Ets-1 (Residues 1−*138).* The DNA sequence encoding Ets-1 (residues 1−138), which was PCR amplified from the full-length murine *ets*-1 cDNA cloned into pET28 (Invitrogen) (*30*), was used to express Ets-1(1−138) as an N-terminal, hexahistidine fusion protein, EtsΔ138 in *E. coli* BL21(DE3) pLysS. The purification of EtsΔ138 has been described previously (*40*).

(2) (His_6-Tagged) MKK1G7B. MKK1G7B was expressed as a His_6-tagged fusion protein in *E. coli* BL21(DE3) pLysS following induction at an OD_{600} of 0.8 with 0.5 mM IPTG. The protein was purified by Ni−NTA affinity chromatography in a manner similar to that described for (His_6-tagged) ERK2 (below), followed by a Mono Q HR 5/5 purification step using a 0 to 500 mM NaCl gradient over the course of 20 min at 1 mL/min. The protein eluted as a peak centered at 255 mM NaCl. Pooled protein fractions were dialyzed at 4 °C into buffer S1A [20 mM HEPES (pH 7.5), 2 mM DTT, 0.1 mM EDTA, 0.1 mM EGTA, 0.05 M KCl, and 5% (v/v) glycerol], concentrated in a Centricon-10 spin column (Amicon, Bedford, MA) at 4 °C to 2 mg/mL, aliquoted, and stored at −80 °C. The enzyme purity was assessed by analyzing the density of Coomassie-stained bands following

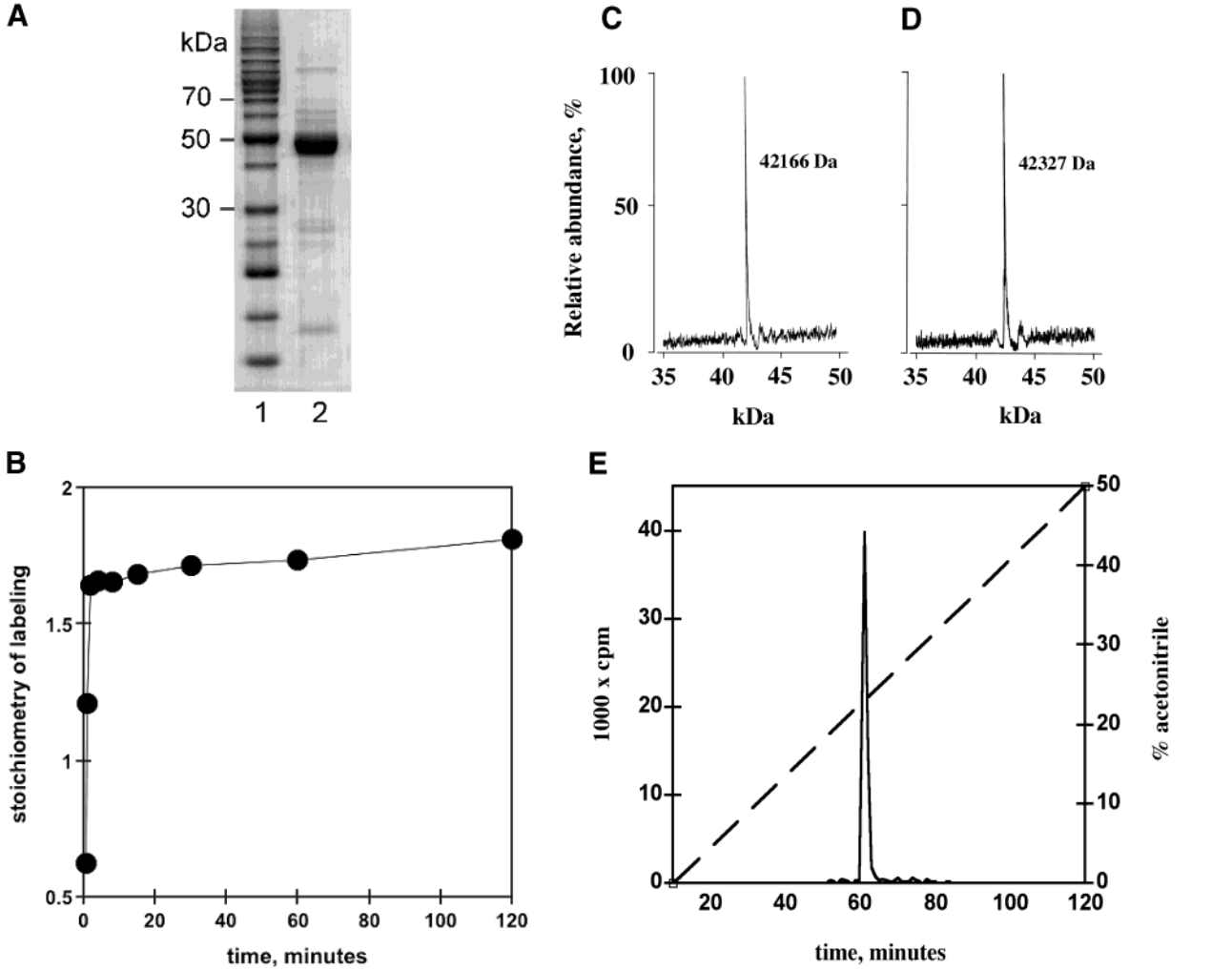

FIGURE 2: Preparation of activated ERK2. (A) SDS−PAGE (12%) of His_6-MKK1G7B: lane 1, molecular mass markers; and lane 2, His_6-MKK1G7B fraction eluted from Mono Q HR 5/5 column. (B) Stoichiometry of phosphorylation of His_6-ERK2 by His_6-MKK1G7B. (C) ESI trace of His_6-ERK2: calculated mass, 42 166 Da; observed mass, 42 166 Da. (D) ESI of activated His_6-ERK2: calculated mass, 42 324 Da; observed mass, 42 327 Da. (E) Isolation of the dual-phosphorylated tryptic peptide of the ERK2 activation loop.

SDS−PAGE (Figure 2A), and by this criterion, it was estimated to be 72% pure.

(3) Activated (His_6-Tagged) ERK2. Inactive rat ERK2 was expressed in *E. coli* BL21(DE3) pLysS and purified as described previously (*1*).[5] A mutant of MKK1 (MKK1G7B), which phosphorylates ERK2 on Thr-183 and Tyr-185, was used to activate the enzyme (*58*). For activation, buffer A2 [20 mM HEPES (pH 7.5), 20 mM $MgCl_2$, 2 mM DTT, 0.1 mM EDTA, 0.1 mM EGTA, 4 mM ATP or [γ-^{32}P]ATP (100−1000 cpm/pmol), and 0.05 M NaCl] was pre-equilibrated in a 27 °C water bath. Frozen stocks of 2 mg/mL ERK2 (10 mg, 245 nmol) in buffer S1 and MKK1G7B (1 mg, 10.5 nmol in buffer S1) were thawed rapidly at 30 °C, centrifuged briefly (2 min at 13 000 rpm), and added to activation buffer A2 (35 mL) to final concentrations of 7 and 0.3 μM, respectively. After 3 h, the mixture was applied to a 1 mL column of DEAE-Sepharose FF (Pharmacia) equilibrated in buffer H1 [20 mM Tris-HCl (pH 8.0), 0.1% (v/v) β-mercaptoethanol, 0.02% (by mass) Brij-30, 0.1 mM EDTA, and 0.1 mM EGTA] containing 0.05 mM NaCl. Elution of ERK2 resulted after 10 mL aliquots of incremental concentrations of NaCl (50 mM increments) in buffer H1 had been applied to the column. Fractions (1 mL) were analyzed for protein using the method of Bradford (*59*). A major protein peak (8−8.5 mg of protein) eluted at 200 mM NaCl, which corresponds to ERK2. The collected fractions were diluted 5-fold and loaded onto a Mono Q HR 10/10 column equilibrated in buffer H1 containing 0.05 mM NaCl. A linear gradient of 4.2 mM/min NaCl at a flow rate of 1.5 mL/min resolved ERK2. Fractions associated with a single peak (A_{280}) at 0.22−0.24 M NaCl were pooled and dialyzed overnight at 4 °C into storage buffer S1. Following dialysis, the protein was concentrated to 2 mg/mL with a Centricon-10 spin column, before being snap frozen in liquid nitrogen and stored at −80 °C.

Site-Directed Mutagenesis. Overlap extension polymerase chain reaction (PCR) methods were used to create the N-terminal hexahistidine-tagged EtsΔ138 S26A construct. pET-28a plasmid-containing DNA for EtsΔ138, inserted at the multiple cloning region between restriction sites for *Nde*I and *Hin*dIII, was used as the template for introduction of

[5] The N-terminus of the expressed enzyme contains the AHHHH-HHAM His_6 tag which is substituted for the N-terminal MA sequence of the wild-type enzyme.

the S26A mutation. The external PCR primers were primer A (5′-GGTGATGCCGGCCACGATGC-3′) and primer B (5′-GCTAGTTATTGCTCAGCGGTGG-3′) which contain *Nde*I and *Hin*dIII restriction sites, respectively. The two internal primers were primer C (5′-CGAGCTTTTCCCT-GCTCCGGACATGGAAT-3′) and primer D (5′-ATTC-CATGTCCGGAGCAGGGAAAAGCTCG-3′). First-round PCR products (P1, template, primer A, and primer D; P2, template, primer B, and primer C) were gel purified and combined with primers A and D before a second round of PCR. The resulting full-length PCR product was digested, purified, and ligated into pET-28a using *Nde*I and *Hin*dIII restriction sites. The ligated product was introduced into *E. coli* DH5α by electroporation, amplified, purified, and sequenced.

Tryptic Analysis of Proteins. Following dialysis against 50 mM Tris (pH 8.65), 250 μg of activated ^{32}P-labeled ERK2 was incubated overnight with 10 μg of sequencing grade trypsin (Roche) at 37 °C (total volume of 200 μL). The digested sample was centrifuged at 13 000 rpm for 10 min, before 100 μL of the supernatant was applied to a 250 mm × 4 mm Vydac 218TP54 C_{18} column (Separations Group, Hesperia, CA) equilibrated with 0.1% TFA (v/v). The column was developed with a linear acetonitrile gradient (0.45% per min) in 0.1% TFA. The flow rate was 0.7 mL/min, and 0.7 mL fractions were collected and analyzed for ^{32}P radioactivity using liquid scintillation counting. Fractions containing radioactivity were analyzed by electrospray mass spectrometry.

Mass Spectrometry. Proteins were analyzed by LC−MS with a Finnigan-MAT LCQ (Finnigan/ThermoQuest, San Jose, CA) electrospray, ion trap mass spectrometer coupled with a Magic 2002 microbore HPLC system (Michrom BioResource, Auburn, CA), housed in the Analytical Instrumentation Facility Core in the College of Pharmacy at the University of Texas at Austin. A 0.5 mm × 50 mm MAGIC MS C_{18} column (particle diameter of 5 μm, pore size of 200 Å) with mobile phase A (2:98:0.1:0.02 acetonitrile/water/acetic acid/trifluoroacetic acid) and mobile phase B (10:90:0.009:0.02 acetonitrile/water/acetic acid/trifluoroacetic acid) was used with 50% B at a flow rate of 20 μL/min. Prior to the analysis, protein samples (typically 0.5 mg for a 43 kDa protein) were cleaned up by reverse phase HPLC using a C_{18} column (Vydac 218TP54, 250 mm × 4 mm) equilibrated in 0.1% TFA and resolved with a linear 0 to 100% gradient of acetonitrile at 0.6 mL/min over 80 min. Protein elution was monitored at 280 nm, and corresponding fractions were combined, lyophilized, and resuspended in 20 μL of 50% acetonitrile containing 0.1% TFA (v/v).

Tryptic digest peptide samples (above) were analyzed on the delayed extraction Voyager-DE PRO MALDI-TOF instrument (PerSeptive Biosystems, Framingham, MA) operating in the positive ion mode. The instrument is equipped with a 337 nm nitrogen laser with a 20 Hz firing rate. The matrix used was α-cyano-4-hydroxycinnamic acid from the Sequazyme Peptide Mass Standards Kit (PerSeptive Biosystems), mixed 1:1 with the sample and drop dried on a stainless steel target in a total volume of 1 μL. Close external calibration was performed using Calibration Mixture 1 (Sequazyme Peptide Mass Standards Kit) made up according to the manufacturer's recommendations. The detector was used with the low mass gate set at *m*/*z* 600, and spectra were acquired over the range of *m*/*z* 600−2500. The data were acquired using an accelerating voltage of 20 kV, a grid voltage of 80%, a guide wire voltage of 0.05%, and an extraction delay time of 225 ns. Up to 400 shots were averaged for the spectrum.

Determination of the ERK2 Protein Concentration. A purified sample of ERK2 was analyzed by three independent methods: (1) Bradford assay (*59*), (2) absorbance measurements at 280 nm, and (3) amino acid analysis. Bradford assays were conducted according to the manufacturer's suggested protocols using a bovine serum albumin standard (Sigma). The extinction coefficient of (His_6-tagged) ERK2 ($\epsilon_{280} = 44\,885\ cm^{-1}\ M^{-1}$) was calculated from the primary sequence and the concentration determined, using this value, by measuring the absorbance at 280 nm in 6 M guanidine chloride following the method of Gill and von Hippel (*60*). The amino acid composition of purified (His_6-tagged) ERK2 was determined by hydrolyzing a sample of the protein in 6 N HCl at 110 °C for 24 h, after which the phenyl isothiocyanate derivatives of the amino acids were synthesized and analyzed on a 420A ABI/PE amino acid analyzer. The whole analysis was performed in triplicate (*61*). The three methods were compared, and a new extinction coefficient (ϵ_{280}) of 52 067 $cm^{-1}\ M^{-1}$ was calculated from the amino acid analysis results. This value was used to determine all ERK2 concentrations in this study.

Steady State Kinetics. Protein kinase assays are conducted at 27 °C in assay buffer A3 [25 mM HEPES (pH 7.5), 50 mM KCl, 2 mM DTT, 0.1 mM EDTA, and 0.1 mM EGTA], containing 2 nM ERK2, 2.5−300 μM EtsΔ138, 2.0−4.0 mM [γ-^{32}P]ATP (100−1000 cpm/pmol), 0.5 μg/mL BSA, and 20 mM $MgCl_2$ in a final volume of 50−100 μL. The pH of the solution is measured both before and after the assay. Reaction mixtures are prepared as follows. Solution S1 is a freshly prepared 10× stock solution of HEPES (pH 7.5), DTT, KCl, EDTA, and EGTA. Solution S2 is a 10× stock of $MgCl_2$. Solution S3 is a 10× stock of EtsΔ138 diluted to the appropriate concentration in a 1× S1. To prepare this, a 1.5 mM stock of EtsΔ138 [in 2.5 mM HEPES (pH 7.5)] is thawed rapidly and serially diluted to the appropriate concentration. Solution S4 is a stock of ATP (pH 7.5). Solution S5 is a 10× stock of ERK2 diluted to the appropriate concentration in a 1× S1 containing BSA (5 μg/mL). To prepare this, a 200 μM sample of ERK2 is thawed rapidly and diluted serially. Solutions S1−S4 and water are combined in a 4*v*:5*v*:5*v*:5*v*:26*v* ratio and incubated for 15 min at 27 °C before initiation of the reaction by the addition of a 5*v* equivalent of pre-equilibrated ERK2 solution S5. Aliquots (5−10 μL) are taken at set time points and applied to 2 cm × 2 cm P81 cellulose paper. The papers are washed (3 × 10 min) in 50 mM phosphoric acid (H_3PO_4) and then in acetone (3 × 1 min) and dried. The amount of labeled protein is determined by counting the associated counts per minute on a Packard 1500 scintillation counter at a σ value of 2.

Rapid Quench Kinetics. All transient kinetics were performed on a Kintek RQF-3 rapid quench-flow apparatus (Kintek Corp., Austin, TX). Reaction mixtures were obtained using the same general approach that was used for the steady state assays. The rapid quench consists of a computer-controlled step motor, a quench syringe, two drive syringes, two sample loading ports, and seven reaction loops of

different lengths. Reactions are initiated by depression of the drive syringes, which forces the reactants together. The reaction mixture then travels through the reaction loop for a given period of time. The reaction is quenched as the mixture exits the reaction loop and is ejected from the apparatus. The desired reaction time is achieved by variation of the reaction loop length and the flow rate of the reaction mixture through the loops. Since these properties vary slightly between machines, the rapid quench-flow apparatus requires a thorough calibration. The calibration process involves two steps: (1) volume quantification of individual reaction and sample loops and (2) calibration of the motor speed. Manufacturer-suggested protocols for calibration were employed. The accuracy of the calibration was verified using a test reaction, the pseudo-first-order base-catalyzed (0.1−1.0 M NaOH) hydrolysis of benzylidene malononitrile (2 mM). Reaction progress was monitored spectrophotometrically (310 nm) at 20 °C. The data were analyzed for continuity between the reaction loops and overall fitting to a single-exponential function. For comparison, the reaction was also conducted under identical conditions in a Kintek SF 2001 stopped-flow apparatus. Both methods produced a similar observed rate constant k_{obs} of 83 ± 3 s^{-1} at 1 M NaOH and 2 mM BMN.

Rapid quench-flow experiments were conducted at 27 °C on a Kintek RQF-3 apparatus. A solution of [γ-^{32}P]ATP (100−1000 cpm/pmol) in buffer A3 containing 20 mM $MgCl_2$ was loaded into sample loop A (14.6 μL). A separate solution containing EtsΔ138 and ERK2 in buffer A3 containing 20 mM $MgCl_2$ was loaded into sample loop B (15.4 μL). For experiments monitoring multiple enzymatic turnovers, final concentrations of 2−4 mM ATP, 150−200 μM EtsΔ138, and 5−5400 nM ERK2 were used. Alternatively, single-turnover experiments were conducted at final concentrations of 2−4 mM ATP, 5−20 μM EtsΔ138, and 158 μM ERK2. Rapid mixing of the reactants was initiated by a computer-controlled step motor, and quenched with 115 μL of 2 M H_3PO_4. The quenched reaction mixture was collected in 1.5 mL centrifuge tubes and centrifuged briefly at 5000*g*. Aliquots (50 μL) of the quenched reaction mixture were spotted on 2 × 2 cm Whatman P81 chromatography paper. The papers were analyzed as described above in Steady State Kinetics. Control experiments were performed to quantify the recovery of the reaction product, EtsΔ138∼P. First, ^{32}P-labeled EtsΔ138∼P was generated by incubation of EtsΔ138 (20 μM) with ERK2 (5 nM) and [γ-^{32}P]ATP (2 mM) in buffer A3 containing 20 mM $MgCl_2$ for 2 h at 27 °C. Buffer was exchanged to remove excess [γ-^{32}P]ATP using a Centricon-10 spin column. The specific recovery of labeled EtsΔ138∼P from the rapid quench apparatus was found to vary from 64 ± 3 to 76 ± 2%, under assay conditions, which depended on the reaction loop that was used.

Data Analysis. All curve fitting was performed using nonlinear regression methods provided by the Kaleidagraph program. Initial rates were typically determined from reaction time courses (using five non-zero time points) by plotting the amount of phosphorylated product (P) formed over time, fitting the data to the single-exponential equation $[P] = A(1 - e^{-kt})$, and then differentiating the resulting curve at time zero (which for this equation is mathematically equivalent to the product *kA*). When the curve of product formation over time was better approximated by a line (as opposed to a single exponential), the curve was fit to the equation $[P] = mx + b$ and the initial reaction rate was then determined from the slope (*m*) of the resulting line. The initial reaction rates were then plotted as a function of substrate concentration and fit to the appropriate steady state equations (*4*). Data in rapid quench experiments were fit to various equations noted in the text.

RESULTS

Activation, Purification, and Analysis of His$_6$-Tagged ERK2. To facilitate purification of ERK2, the protein is expressed in *E. coli* BL21(DE3) pLysS as described in Materials and Methods. It is then activated *in vitro* by a constitutively active form of MKK1 termed MKK1G7B (*58*), which is also expressed as an N-terminal hexahistidine fusion protein. Since full activation of ERK2 requires phosphorylation on both Thr-183 and Tyr-185, the specificity of phosphorylation on these two residues was determined as the main criterion for determining the integrity of the activation. Thus, in addition to protein mass spectrometry, which determines the stoichiometry of phosphorylation, the homogeneity of the enzyme preparation was determined by a regiospecific analysis of its phosphorylation state. The ability of reverse phase HPLC to separate phospho isoforms of tryptic peptide fragments provided the basis for the analysis.

The His$_6$-MKK1G7B isolated from bacterial lysate by Ni^{2+} agarose affinity chromatography was further purified by anion exchange chromatography using a Mono Q HR 5/5 column, developed with a 0 to 500 mM NaCl gradient over the course of 20 min. The peak corresponding to His$_6$-MKK1G7B eluted at 255 mM NaCl (data not shown) and was judged to be 72% pure and suitable for the activation of His$_6$-ERK2. Efficient activation of His$_6$-ERK2 was achieved by incubating His$_6$-MKK1G7B (300 nM) with His$_6$-ERK2 (7 μM) and $MgATP^{2-}$ (4 mM) in the presence of 16 mM free Mg^{2+} at pH 7.5 for 2−3 h. At the concentrations that were used, phosphorylation occurs to a stoichiometry approaching 1.7 mol/mol within 40 min (Figure 2B). While prolonged incubation beyond 3 h leads to a higher overall stoichiometry of phosphorylation, it also leads to the appearance of tris-phosphorylated species. As we cannot separate bis- and tris-phosphorylated ERK2 on the Mono-Q column, we limited the activation time to less than 3 h, which prevents the formation of significant tris-phosphorylated species. The phosphorylated protein was purified by DEAE-Sepharose FF chromatography, followed by Mono-Q HR 10/10 chromatography, with an overall yield of 85%. The Mono-Q column was developed with a 0 to 500 mM NaCl gradient over the course of 80 min, which resulted in elution of bis-phosphorylated ERK2 at 230 mM NaCl (data not shown). Since His$_6$-MKK1G7B elutes at 255 mM NaCl, it should be noted that the final preparation of active His$_6$-ERK2 could contain trace amounts of MKK1G7B. Using SDS−PAGE analysis and band density measurements as a criterion, no MKK1G7B was detected and the active His$_6$-ERK2 was estimated to be more that 95% pure. The concentration of ERK2 was determined by amino acid analysis, the most direct method available for deriving an extinction coefficient ϵ_{280} of 52 067 cm^{-1} M^{-1} for the expressed protein.

Phosphorylation of ERK2 was confirmed by electrospray mass spectrometry, which revealed an increase in mass of 161 Da from 42 166 (Figure 2C) to 42 327 Da (Figure 2D). To identify the sites of phosphorylation, radiolabeled His_6-ERK2 was trypsinized. The tryptic peptides were then resolved by reverse phase HPLC and individual fractions analyzed for ^{32}P content by liquid scintillation counting. All the ^{32}P associated with the protein eluted as a single peak at 24% (v/v) acetonitrile and 0.1% TFA (Figure 2E). Peak fractions containing ^{32}P were analyzed by MALDI and contained a single 2306.2 Da peptide. This corresponds to the calculated mass (2307.3 Da) of the doubly phosphorylated tryptic peptide ^{171}VADPDHDHTGFLTEYVATR^{189}. Phosphoamino acid analysis of the purified phosphopeptide (not shown) confirmed the expected presence of both a phosphorylated threonine and tyrosine. While phosphorylation of Thr-179 or Thr-188 is not rigorously excluded by this analysis, neither phosphorylation has been observed before. It is noteworthy that an active site titration with 5-iodotubericidin indicates that 95% of the activated protein can bind the inhibitor (*1*). This suggests that 95 ± 10% of the bis-phosphorylated enzyme is active.

Characterization of EtsΔ138 S26A. To probe the mechanism and undertake structure−function studies of ERK2 requires protein substrates. Currently, the best available substrate for ERK2 is comprised of residues 1−138 of transcription factor Ets-1 (*1*). This region encompasses a highly conserved domain within the *Ets* family of transcription factors, termed the pointed (PNT) domain, which contains a putative docking site for ERK2 (*22*). Docking sites are believed to regulate numerous aspects of ERK2 biology, and therefore, this protein provides the means of critically analyzing fundamental aspects of an ERK2 docking site interaction, such as the promotion of Thr-38 phosphorylation, which lies in the disordered N-terminal region of Ets-1 (Figure 1). To avoid potential problems, Ser-26, which is a minor phosphorylation site (under forcing conditions), was mutated to alanine. After phosphorylation of the resultant protein EtsΔ138 Ser26Ala by ERK2, the protein was found to be kinetically indistinguishable from wild-type EtsΔ138 under steady state conditions (data not shown). This protein was therefore employed as the ERK2 substrate for pre-steady state kinetic studies and is termed EstΔ138 in the text.

Transient Kinetic Analysis of ERK2. Rapid quench techniques were used to examine kinetic transients on the catalytic reaction pathway of ERK2. Experiments were performed on a RQF-3 Quench-Flow apparatus as described in Materials and Methods. The apparatus allows measurement of individual points for a reaction time course on the millisecond to second time scale. When reaction progress is monitored using this technique, intermediate complexes are often detected by virtue of changes in the *rate* of product or substrate concentration. To analyze the mechanism of ERK2, the formation of EtsΔ138∼P was monitored in buffer A3 containing 20 mM $MgCl_2$. For each reaction, ERK2 (1.8−10.0 μM) was preincubated with saturating EtsΔ138 (300−400 μM) before rapid mixing with an equal volume of ATP^{4-} (4−8 mM). After a designated period (2−150 ms), reactions were quenched with acid via a second mixing event. ^{32}P-labeled EtsΔ138∼P was then recovered and quantified after calibration of the machine as described in Materials and Methods.

Scheme 1

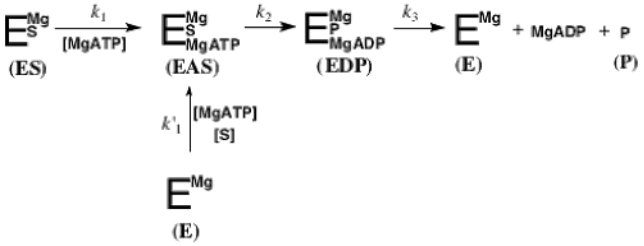

$$\frac{[EDP]+[P]}{[E]_0} = \alpha(1 - e^{-k_b t}) + k_{cat}^{D} t \quad (1)$$

$$\alpha = \left(\frac{k_2}{k_2 + k_3}\right)^2 \quad (2)$$

$$k_b = k_2 + k_3 \quad (3)$$

$$k_{cat} = \frac{k_2 k_3}{k_2 + k_3} \quad (4)$$

$$\frac{[EDP]+[P]}{[E]_0} = \left(\frac{k_2}{k_2 + k_3}\right)^2 [1 - e^{-(k_2+k_3)t}] + \left(\frac{k_2 k_3}{k_2 + k_3}\right) t \quad (5)$$

Figure 3A depicts four time courses, for the formation of EtsΔ138∼P, obtained at different concentrations of ERK2 (0.70, 1.40, 2.80, or 4.21 μM). Each time course is characterized by an initial burst followed by a slower, linear phase. This corresponds to exponential and linear segments described by eq 1 for a pre-steady state burst mechanism according to the simplified kinetic model shown in Scheme 1.[6] According to this model, ERK2 is initially complexed to EtsΔ138, in the presence of 20 mM magnesium ion. The binding of $MgATP^{2-}$ to the preformed complex, ES, to form EAS, k_1, is assumed to be fast (>345 s^{-1})[7] and irreversible under the conditions that are employed (2 mM $MgATP^{2-}$ and 20 mM total Mg^{2+}). Thus, according to this model, the reaction rate is dependent on two irreversible steps: the rate of product formation on the enzyme, k_2, and the rate of product release from the enzyme, k_3.

Equation 1 was derived assuming that EtsΔ138 is saturating under the conditions of the experiment, an assumption supported by the observation that variations in the concentration of EtsΔ138 (150−200 μM) have no discernible effect on the rate of appearance of EDP and P (Table 1). These experiments also support the notion that the binding of $MgATP^{2-}$ (k_1) is rapid (>0.69/t* s^{-1}), because slow addition would produce an initial lag in product formation.[8] When both substrates [EtsΔ138 (300 μM) and $MgATP^{2-}$ (4 mM)]

[6] In this scheme, the phosphorylation of EtsΔ138, k_2, is assumed to be irreversible. Significantly, the overall reverse reaction is considerably slower (>1000-fold) than the forward reaction (W. F. Waas, K. Cox, and K. N. Dalby, unpublished observations), and furthermore, the inclusion of a significant reversible step impairs the fit to the transient data.

[7] This corresponds to a half-life of 2 ms, the dead time (t*) of the rapid quench apparatus. Approximately 50% of a first-order process with a rate constant k of 345 s^{-1} would be complete within the dead time of the instrument.

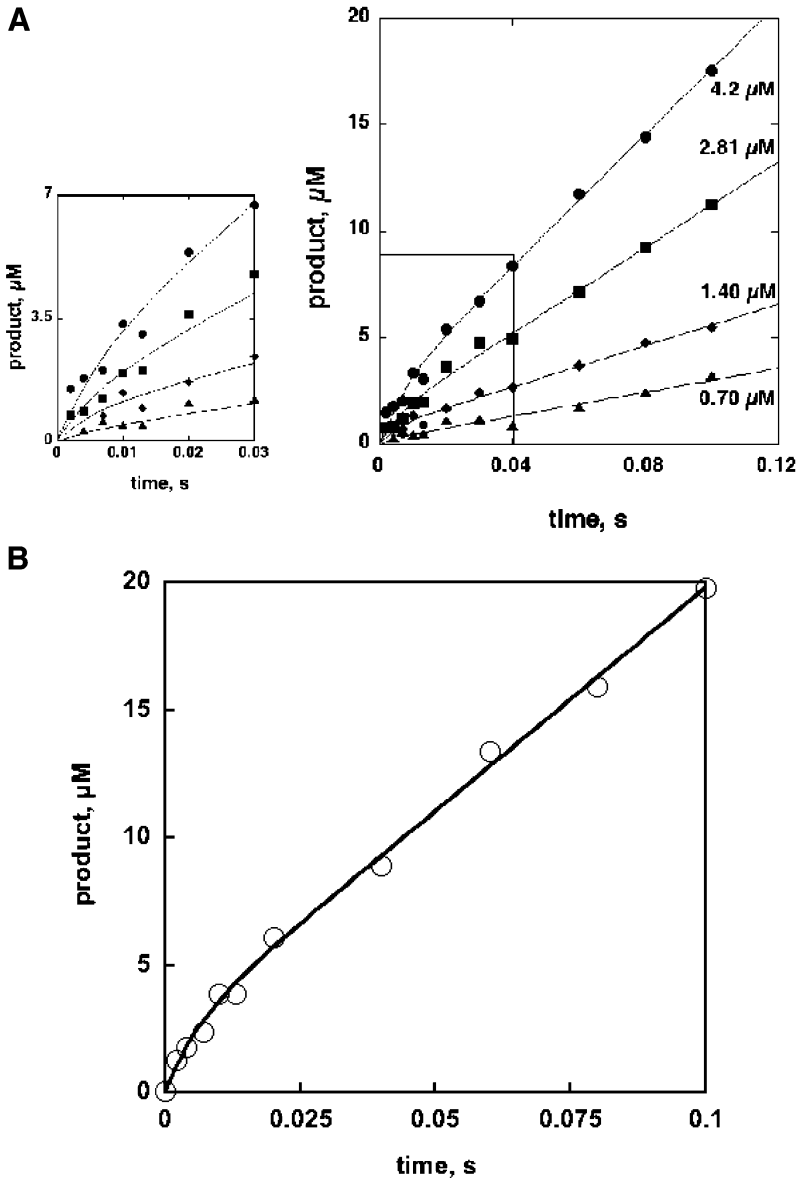

FIGURE 3: (A) Rapid mixing of $MgATP^{2-}$ with ERK2·EtsΔ138. Rapid quench-flow experiments were conducted at 27 °C and pH 7.5 in buffer A3 (25 mM HEPES, 50 mM KCl, 2 mM DTT, 0.1 mM EDTA, and 0.1 mM EGTA) containing 20 mM $MgCl_2$. [γ-^{32}P]ATP (100−1000 cpm/pmol) was loaded into sample loop A, while proteins EtsΔ138 and ERK2 were loaded into sample loop B. Final concentrations were 2 mM $MgATP^{2-}$, 150 μM EtsΔ138, and 0.7 (▲), 1.4 (■), 2.8 (◆), and 4.21 μM ERK2 (●). At set times, reactions were quenched by the addition of 2 M H_3PO_4 and product formation (EDP + P, Scheme 1) was quantified as described in Materials and Methods. The lines through the data correspond to the best fit to eq 5 according to a k_2 of 109 s^{-1} and a k_3 of 56 s^{-1}. (B) Rapid mixing of ERK2 with EtsΔ138 and $MgATP^{2-}$. The experiment was conducted in a manner identical to that of the experiment described above, except that EtsΔ138 and $MgATP^{2-}$ were incubated together in sample loop A, prior to the rapid mixing with ERK2 from sample loop B. Final concentrations were 2 mM ATP, 150 μM EtsΔ138, and 4.9 μM ERK2. The lines through the data correspond to the best fit to eq 5 according to a k_2 of 109 s^{-1} and a k_3 of 56 s^{-1}.

are preincubated together in syringe A before being mixed with an equal volume of ERK2 (9.8 μM), the rate of appearance of EDP and P (Figure 3B) is essentially indistinguishable from the experiment shown in Figure 3A where EtsΔ138 is preincubated with ERK2. This experiment indicates that the binding of 150 μM EtsΔ138, through the lower pathway shown in Scheme 1 (k'_1), is also fast, with a rate constant of $>0.69/t^*$ s^{-1}.

[8] The second-order rate constant for the binding of $MgATP^{2-}$ to protein kinases is typically greater than 1×10^5 M^{-1} s^{-1} and has been estimated to be greater than 2×10^6 M^{-1} s^{-1} for the binding to the ERK2·MBP binary complex (*3*).

Equation 1 has three independent variables, α, k_b, and k_{cat}. The amplitude α and the rate constant k_b determine the magnitude and rate of accumulation of EDP from EAS, while the catalytic turnover, k_{cat}, represents the rate of conversion of EAS to E. These parameters are defined by rate constants k_2 and k_3 according to eqs 2−4. The appropriate substitution of eqs 2−4 into eq 1 gives eq 5, which has two independent variables (k_2 and k_3) and is used to analyze individual burst experiments. The analyses of several experiments over a range of enzyme and substrate conditions are in good agreement and are reported in Table 1. From these values, the amplitude α, the burst rate constant k_b, and the catalytic

Table 1: Pre-Steady State Kinetic Parameters Obtained from Burst Experiments[a]

[ERK2] (μM)[d]	[EtsΔ138] (μM)[e]	k_2[f] (s^{-1})	k_3[f] (s^{-1})
0.70[b]	150	95 ± 33	68 ± 27
1.40[b]	150	137 ± 28	50 ± 6
2.08[b]	238	94 ± 6	53 ± 3
2.80[b]	150	106 ± 12	54 ± 5
3.70[b]	238	119 ± 16	61 ± 6
4.21[b]	150	118 ± 12	55 ± 4
4.90[c]	150	111 ± 9	52 ± 4

[a] Rapid quench-flow experiments were conducted at pH 7.5 in buffer A3 (25 mM HEPES, 50 mM KCl, 2 mM DTT, 0.1 mM EDTA, and 0.1 mM EGTA) containing 20 mM $MgCl_2$ at 27 °C. Quenched reactions (2 M H_3PO_4) were analyzed as described in Materials and Methods. [b] [γ-^{32}P]ATP (100−1000 cpm/pmol; final concentration of 2 mM) was rapidly mixed with a pre-equilibrated solution of EtsΔ138 and ERK2 before quenching. [c] ERK2 was mixed with a pre-equilibrated solution of EtsΔ138 and [γ-^{32}P]ATP (100−1000 cpm/pmol; final concentration of 2 mM) before quenching. [d] Determined using an extinction coefficient ϵ_{280} of 52 067 cm^{-1} M^{-1}. [e] Determined using an extinction coefficient ϵ_{280} of 23 231 cm^{-1} M^{-1} (*40*). [f] Obtained from a nonlinear least-squares fit of [EDP] + [P] vs time according eq 5. Errors are standard deviations.

Table 2: Phosphorylation of EtsΔ138 under Single-Turnover Conditions[a]

[ERK2] (μM)[b]	[EtsΔ138][c] (μM)	k_2[d] (s^{-1})	end point[b] (μM)
158	20	110.5 ± 13.6	19.0 ± 0.7
158	15	130.2 ± 16.1	16.1 ± 0.5
158	10	79.2 ± 13.8	9.2 ± 0.5

[a] Rapid quench-flow experiments were conducted at pH 7.5 in buffer A3 (25 mM HEPES, 50 mM KCl, 2 mM DTT, 0.1 mM EDTA, and 0.1 mM EGTA) containing 20 mM $MgCl_2$ at 27 °C. Quenched reactions (2 M H_3PO_4) were analyzed as described in Materials and Methods. [γ-^{32}P]ATP (100−1000 cpm/pmol; final concentration of 2 mM) was rapidly mixed with a pre-equilibrated solution of EtsΔ138 and ERK2 before quenching. [b] Determined using an extinction coefficient ϵ_{280} of 52 067 cm^{-1} M^{-1}. [c] Determined using an extinction coefficient ϵ_{280} of 23 231 cm^{-1} M^{-1} (*40*). [d] Obtained from a nonlinear least-squares fit of [EDP] + [P] vs time according eq 6. Errors are standard deviations.

constant k_{cat} can be calculated. The averaged values over all the experiments are as follows: $\alpha = 0.44$, $k_b = 164$ s^{-1}, and $k_{cat} = 37$ s^{-1}. These are in good agreement with a k_2 value of 109 ± 9 s^{-1} and a k_3 value of 56 ± 4 s^{-1}, which were obtained by a global analysis, according to eq 5, of all the burst data obtained in one experiment at 150 μM EtsΔ138.

Single-Turnover Experiments. The analysis described above is critically dependent on the determination of the active site concentration. Although a previous active site titration using isothermal calorimetry to follow the binding of 5-iodotubericidin to ERK2 suggested that the active site concentration is in line with the amino acid analysis (*1*), we sought further evidence to support this. Thus, the phosphorylation of EtsΔ138 by ERK2 was analyzed under single-turnover conditions. Under these conditions, because EtsΔ138 is limiting, and k_3 is kinetically transparent, the experiment directly assesses the formation of EtsΔ138∼P on the enzyme. Thus, according to Scheme 1, after rapid mixing of ERK2·EtsΔ138 and $MgATP^{2-}$ (k_1) under single-turnover conditions, the appearance of product is limited by k_2 alone. As this analysis makes no assumption about the concentration of ERK2 (because the appearance of product is independent of the concentration of ERK2), it provides an independent determination of k_2, which can be compared to the value obtained in the burst experiments.

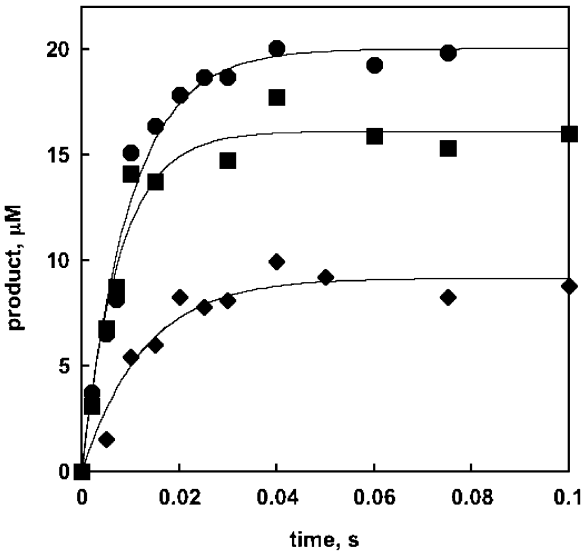

FIGURE 4: Formation of EtsΔ138∼P when ERK2 is in excess. Rapid quench-flow experiments were conducted at 27 °C and pH 7.5 in buffer A3 (25 mM HEPES, 50 mM KCl, 2 mM DTT, 0.1 mM EDTA, and 0.1 mM EGTA) containing 20 mM $MgCl_2$. [γ-^{32}P]-ATP (100−1000 cpm/pmol) was loaded into sample loop A, while proteins EtsΔ138 and ERK2 were loaded into sample loop B. At set times, the reactions were quenched by the addition of 2 M H_3-PO_4 and product formation (EDP + P, Scheme 1) was quantified as described in Materials and Methods. The lines through the circles correspond to the best fit to eq 6 according to a k_2 of 106 s^{-1}.

ERK2 (300 μM) was preincubated with EtsΔ138 (20−40 μM) in buffer A3 containing 20 mM Mg^{2+}, before rapid mixing with an equivalent volume of $MgATP^{2-}$ (8 mM) in the same buffer (20 mM total Mg^{2+}). The formation of EDP was then monitored from 2 to 75 ms. Under these conditions, it is assumed that initially EtsΔ138 is fully complexed to ERK2 and that $MgATP^{2-}$ binding is rapid. As the dissociation constant for the ERK2·EtsΔ138 complex (ES) has not been measured directly in the presence of 20 mM Mg^{2+}, we used the K_i value of 9 μM, obtained from steady state experiments, as a guide (*4*). On the basis of this value, approximately 93% of EtsΔ138 is predicted to be complexed to ERK2.[9]

$$[EDP]_t = ([EDP]_\infty - [EDP]_0)(1 - e^{-k_2 t}) \qquad (6)$$

As predicted, the appearance of EtsΔ138∼P, under the single-turnover conditions, is exponential (Figure 4). In each case, the resulting time course is described by a single-exponential function that conforms to within 10% of the theoretical end point. According to the model in Scheme 1, the rapid formation of EAS (k_1) is followed by the rate-limiting formation of EDP (k_2). The best nonlinear fits through the experimental data, according to eq 6, obtained at three EtsΔ138 concentrations (10−20 μM, final) correspond to an average k_2 value of 106 ± 25 s^{-1}. The good first-order fit to the experimental data, and the close agreement between the actual and predicted end point, support the assumptions of Scheme 1. Notably, the k_2 value of 106 ± 25 s^{-1} is in good agreement with the k_2 value of 109 ± 9 s^{-1} derived from the burst analysis.

[9] This is calculated from the quadratic equation $[ES]/[E]_0 = \langle E_0 + S_0 + K_d - (E_0 + S_0 + K_d)^2 - 4E_0S_0\rangle/2E_0$, where $[E]_0 = [E] + [ES]$ and $[S]_0 = [S] + [ES]$.

DISCUSSION

Given its central role in mitogenic signaling, an understanding of the catalytic mechanism and regulation of ERK2 is essential in appreciating the implications of potential inhibitors and the consequences of both protein−protein interactions and allele variations within cells. This stance was the basis for setting out to characterize the steady state kinetic mechanisms of ERK2 and other MAP kinases (*1*, *4*, *40*, *62*). Of course, steady state experiments are limited because individual steps are often transparent to the analysis; therefore, we chose to pursue a transient kinetic approach also. In this respect, active ERK2 represented a challenging prospect, because it must be prepared in a fully modified form to be active. To our knowledge, this report represents the first description of a transient kinetic study of an enzyme whose activity is dependent on phosphorylation by a second enzyme.

In response to mitogenic stimuli, MAPKK1 and -2 phosphorylate ERK2 on Thr-183 and Tyr-185. The covalently bound phosphates stabilize a conformation of the enzyme that is conducive to catalysis, notably, through closure of the two domains that create the active site, realignment of catalytic residues, and the formation of a putative proline binding pocket (*63*). Phosphorylation enhances the catalytic constant of ERK2 some 4 orders of magnitude, promotes recognition of nucleotide and protein substrates (*31*), and is reported to induce homodimerization. Its role in promoting nuclear uptake is controversial (*54*, *64*−*66*).

Purification of Bis-Phosphorylated ERK2. The purification of *inactive* His_6-ERK2 described in this report utilizes a Ni^+ affinity purification/enrichment step to separate it from the majority of the bacterial cell's proteins and ion exchange chromatography to purify it further. Using the methods described above, the presence of small amounts of the monophosphorylated protein can be *quantitatively* revealed.

Reaction Pathway. Previously, the rate-limiting step for the phosphorylation of myelin basic protein (MBP) by ERK2 was reported to be a viscosity insensitive step that was assumed to be phosphoryl transfer (*3*). Therefore, we were surprised to observe a burst of product when $MgATP^{2-}$ was rapidly mixed with ERK2 and EtsΔ138 in the presence of saturating free magnesium ion (Figure 3A). The burst and single-turnover experiments support a mechanism where the phosphorylation of EtsΔ138 by ERK2 is limited by two partially rate-determining steps, k_2 and k_3 (Scheme 1), and show that phosphoryl transfer on ERK2 can occur at least 1 order of magnitude faster than previously realized. Further experiments are required to determine whether k_2 corresponds to phosphoryl transfer or a protein conformational change of either the enzyme or substrate. The second partially rate-limiting step, k_3, corresponds to events that occur after phosphoryl transfer and may be attributed to dissociation of one or both products, any conformational changes associated with such steps, or even a conformational change of the free enzyme after product release. For a number of protein kinases, the rate-limiting step is reported to involve the dissociation of ADP (*50*, *52*, *67*). Notably, in these cases, a peptide substrate was used. Peptide substrates of ERK2 display a significantly higher K_m than the natural protein substrates from which they are derived, and therefore, it is not unreasonable to expect this to be reflected in the steps governing product release. Clearly, because of the intriguing method of substrate recognition employed by ERK2, where most of the thermodynamic stability for the ERK2−protein substrate complex is believed to originate from loci outside of the active site, the use of a well-characterized protein substrate is essential (*25*−*27*). In this respect, it is notable that the affinity of EtsΔ138 for ERK2 is only marginally affected by phosphorylation on Thr-38,[10] and furthermore, phosphorylated EtsΔ138 actually binds tighter to ERK2 than MgADP (*4*). This is significant because, generally, phosphorylated peptide substrates of protein kinase are reported to bind weakly. Thus, it is possible that in the case of ERK2 the dissociation of EtsΔ138∼P actually limits k_3 and not the dissociation of ADP (*4*). Further work is necessary to characterize k_3.

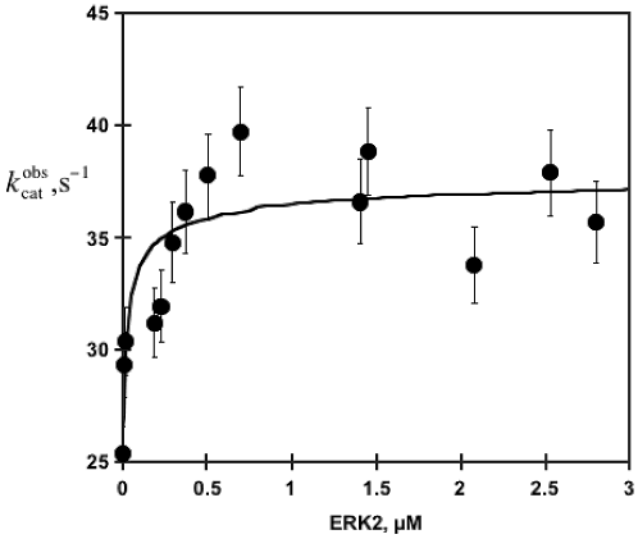

FIGURE 5: Dependence of catalytic turnover, k_{cat}, on the concentration of ERK2. The linear dependence of product formation on time was analyzed several milliseconds after mixing, once steady state turnover was attained, on a Kintek RQF-3 rapid quench-flow apparatus. Assays were conducted at 27 °C and pH 7.5 in assay buffer A3 (25 mM HEPES, 50 mM KCl, 2 mM DTT, 0.1 mM EDTA, and 0.1 mM EGTA) containing 3−4210 nM ERK2, 150 μM EtsΔ138, 2.0 mM [γ-^{32}P]ATP (100−1000 cpm/pmol), 0.5 μg/mL BSA, and 20 mM $MgCl_2$ in a final volume of 50−100 μL. The line through the data corresponds to the best fit according to eq 7 where k_{cat}^{M} and k_{cat}^{D} were fixed at 25 and 37 s^{-1}, respectively.

The reaction pathway appears to differ in several respects from that reported by Prowse *et al.* (*3*). They concluded from steady state solvent viscosity experiments that phosphoryl transfer to both myelin basic protein MBP ($k_p = 14\ s^{-1}$) and the peptide ATGPL<u>SP</u>GPFGRR (ERKtide) ($k_p = 6.5\ s^{-1}$) limits turnover. Until they are verified by rapid quench studies, it is difficult to evaluate the differences. Possible reasons include differences in the enzyme preparations, the substrates employed, or the nature of the active enzyme species (monomers or dimers) in the assays. The latter point is especially relevant because we observe an ERK2-dependent increase in k_{cat} (1.5-fold) (Figure 5), which may reflect a sensitivity of one or more steps to the concentration of ERK2.

[10] EtsΔ138∼P is a competitive inhibitor toward EtsΔ138 with a K_{iC}^{app} of 26 μM at 267 μM ATP and 10 mM Mg^{2+} (*4*).

Toward a Catalytic Mechanism. EtsΔ138 is a protein substrate with significant secondary and tertiary structure, which is phosphorylated by ERK2 through a random-order ternary complex mechanism (*4*). An NMR study of EtsΔ138 shows that Thr-38, the phosphorylation site, is located in a highly flexible region of the protein a significant distance (>20 Å) from Phe-120 (*30*), the site thought to mediate interactions between ERK2 and EtsΔ138 (*22*). The kinetic analysis presented here indicates that two EtsΔ138 substrate molecules can bind per ERK2 dimer and that phosphorylation occurs at each active site with a rate constant k_2 of 109 ± 9 s^{-1} followed by product release with a rate constant k_3 of 56 ± 4 s^{-1}. Recently, we showed that once ERK2 has been primed by Thr-183 and Tyr-185 phosphorylation it is activated by a second magnesium ion (*1*). The mechanism by which magnesium activates the phosphorylated enzyme has not been delineated. The ability to analyze ERK2 using a pre-steady state approach in conjunction with ongoing structural studies should facilitate a better understanding of this fascinating enzyme.

ACKNOWLEDGMENT

We are indebted to Dr. Melanie Cobb, Dr. Natalie Ahn, and Dr. Lawrence McIntosh for generously providing us with DNA encoding His_6-ERK2, MKK1G7B, and His_6-Ets-1(1−138), respectively. Electrospray ionization (ESI) and matrix-assisted laser desorption ionization (MALDI) mass spectrometry was performed in part by the Analytical Instrumentation Facility Core (College of Pharmacy, The University of Texas at Austin) supported by Center Grant ES 07784.

REFERENCES

1. Waas, W. F., and Dalby, K. N. (2003) Physiological Concentrations of Divalent Magnesium Ion Activate the Serine/Threonine Specific Protein Kinase ERK2, *Biochemistry 42*, 2960−2970.
2. Maegley, K. A., Admiraal, S. J., and Herschlag, D. (1996) Ras-catalyzed hydrolysis of GTP: a new perspective from model studies, *Proc. Natl. Acad. Sci. U.S.A. 93*, 8160−8166.
3. Prowse, C. N., Hagopian, J. C., Cobb, M. H., Ahn, N. G., and Lew, J. (2000) Catalytic reaction pathway for the mitogen-activated protein kinase ERK2, *Biochemistry 39*, 6258−6266.
4. Waas, W. F., and Dalby, K. N. (2002) Transient Protein−Protein Interactions and a Random-ordered Kinetic Mechanism for the Phosphorylation of a Transcription Factor by Extracellular-regulated Protein Kinase 2, *J. Biol. Chem. 277*, 12532−12540.
5. Nottage, M., and Siu, L. L. (2002) Rationale for Ras and raf-kinase as a target for cancer therapeutics, *Curr. Pharm. Des. 8*, 2231−2242.
6. Yang, J., Yu, Y., and Duerksen-Hughes, P. J. (2003) Protein kinases and their involvement in the cellular responses to genotoxic stress, *Mutat. Res. 543*, 31−58.
7. Fan, M., and Chambers, T. C. (2001) Role of mitogen-activated protein kinases in the response of tumor cells to chemotherapy, *Drug Resist. Updates 4*, 253−267.
8. Lewis, T. S., Shapiro, P. S., and Ahn, N. G. (1998) Signal transduction through MAP kinase cascades, *Adv. Cancer Res. 74*, 49−139.
9. Pearson, G., Robinson, F., Beers Gibson, T., Xu, B. E., Karandikar, M., Berman, K., and Cobb, M. H. (2001) Mitogen-activated protein (MAP) kinase pathways: regulation and physiological functions, *Endocr. Rev. 22*, 153−183.
10. Avruch, J., Khokhlatchev, A., Kyriakis, J. M., Luo, Z., Tzivion, G., Vavvas, D., and Zhang, X. F. (2001) Ras activation of the Raf kinase: tyrosine kinase recruitment of the MAP kinase cascade, *Recent Prog. Horm. Res. 56*, 127−155.
11. Hoshino, R., Chatani, Y., Yamori, T., Tsuruo, T., Oka, H., Yoshida, O., Shimada, Y., Ari-i, S., Wada, H., Fujimoto, J., and Kohno, M. (1999) Constitutive activation of the 41-/43-kDa mitogen-activated protein kinase signaling pathway in human tumors, *Oncogene 18*, 813−822.
12. Clark-Lewis, I., Sanghera, J. S., and Pelech, S. L. (1999) Definition of a consensus sequence for peptide substrate recognition by p44mpk, the meiosis-activated myelin basic protein kinase, *J. Biol. Chem. 266*, 15180−15184.
13. Sharrocks, A. D., Yang, S. H., and Galanis, A. (2000) Docking domains and substrate-specificity determination for MAP kinases, *Trends Biochem. Sci. 25*, 448−453.
14. Biondi, R. M., and Nebreda, A. R. (2003) Signalling specificity of Ser/Thr protein kinases through docking site-mediated interactions, *Biochem. J. 372*, 1−13.
15. Yang, S. H., Whitmarsh, A. J., Davis, R. J., and Sharrocks, A. D. (1998) Differential targeting of MAP kinases to the ETS-domain transcription factor Elk-1, *EMBO J. 17*, 1740−1749.
16. Yang, S. H., Yates, P. R., Whitmarsh, A. J., Davis, R. J., and Sharrocks, A. D. (1998) The Elk-1 ETS-domain transcription factor contains a mitogen-activated protein kinase targeting motif, *Mol. Cell. Biol. 18*, 710−720.
17. Yang, S. H., Galanis, A., and Sharrocks, A. D. (1999) Targeting of p38 mitogen-activated protein kinases to MEF2 transcription factors, *Mol. Cell. Biol. 19*, 4028−4038.
18. Jacobs, D., Glossip, D., Xing, H., Muslin, A. J., and Kornfeld, K. (1999) Multiple docking sites on substrate proteins form a modular system that mediates recognition by ERK MAP kinase, *Genes Dev. 13*, 163−175.
19. Gavin, A. C., and Nebreda, A. R. (1999) A MAP kinase docking site is required for phosphorylation and activation of p90(rsk)/MAPKAP kinase-1, *Curr. Biol. 9*, 281−284.
20. Smith, J. A., Poteet-Smith, C. E., Lannigan, D. A., Freed, T. A., Zoltoski, A. J., and Sturgill, T. W. (2000) Creation of a stress-activated p90 ribosomal S6 kinase. The carboxyl-terminal tail of the MAPK-activated protein kinases dictates the signal transduction pathway in which they function, *J. Biol. Chem. 275*, 31588−31593.
21. Galanis, A., Yang, S. H., and Sharrocks, A. D. (2001) Selective targeting of MAPKs to the ETS domain transcription factor SAP-1, *J. Biol. Chem. 276*, 965−973.
22. Seidel, J. J., and Graves, B. J. (2002) An ERK2 docking site in the Pointed domain distinguishes a subset of ETS transcription factors, *Genes Dev. 16*, 127−137.
23. Barsyte-Lovejoy, D., Galanis, A., and Sharrocks, A. D. (2002) Specificity determinants in MAPK signaling to transcription factors, *J. Biol. Chem. 277*, 9896−9903.
24. Fantz, D. A., Jacobs, D., Glossip, D., and Kornfeld, K. (2001) Docking sites on substrate proteins direct extracellular signal-regulated kinase to phosphorylate specific residues, *J. Biol. Chem. 276*, 27256−27265.
25. Tanoue, T., Adachi, M., Moriguchi, T., and Nishida, E. (2000) A conserved docking motif in MAP kinases common to substrates, activators and regulators, *Nat. Cell Biol. 2*, 110−116.
26. Tanoue, T., Maeda, R., Adachi, M., and Nishida, E. (2001) Identification of a docking groove on ERK and p38 MAP kinases that regulates the specificity of docking interactions, *EMBO J. 20*, 466−479.
27. Tanoue, T., and Nishida, E. (2002) Docking interactions in the mitogen-activated protein kinase cascades, *Pharmacol. Ther. 93*, 193−202.
28. Chang, C. I., Xu, B. E., Akella, R., Cobb, M. H., and Goldsmith, E. J. (2002) Crystal structures of MAP kinase p38 complexed to the docking sites on its nuclear substrate MEF2A and activator MKK3b, *Mol. Cell 9*, 1241−1249.
29. Tanoue, T., and Nishida, E. (2003) Molecular recognitions in the MAP kinase cascades, *Cell Signalling 15*, 455−462.
30. Slupsky, C. M., Gentile, L. N., Donaldson, L. W., Mackereth, C. D., Seidel, J. J., Graves, B. J., and McIntosh, L. P. (1998) Structure of the Ets-1 pointed domain and mitogen-activated protein kinase phosphorylation site, *Proc. Natl. Acad. Sci. U.S.A. 95*, 12129−12134.
31. Prowse, C. N., and Lew, J. (2001) Mechanism of activation of ERK2 by dual phosphorylation, *J. Biol. Chem. 276*, 99−103.
32. Prowse, C. N., Deal, M. S., and Lew, J. (2001) The complete pathway for catalytic activation of the mitogen-activated protein kinase, ERK2, *J. Biol. Chem. 276*, 40817−40823.
33. Zhou, B., and Zhang, Z. Y. (2002) The activity of the extracellular signal-regulated kinase 2 is regulated by differential phosphorylation in the activation loop, *J. Biol. Chem. 277*, 13889−13899.

34. Lew, J. (2003) MAP Kinases and CDKs: Kinetic Basis for Catalytic Activation, *Biochemistry 42*, 849−856.
35. Hanks, S. K., Quinn, A. M., and Hunter, T. (1988) The protein kinase family: conserved features and deduced phylogeny of the catalytic domains, *Science 241*, 42−52.
36. Guthrie, R. D., and Jencks, W. P. (1989) IUPAC recommendations for the representation of reaction mechanisms, *Acc. Chem. Res. 22*, 343−349.
37. Williams, N. H. (2000) Magnesium Ion Catalyzed ATP Hydrolysis, *J. Am. Chem. Soc. 122*, 12023−12024.
38. Choe, J.-Y., Iancu, C. V., Fromm, H. J., and Honzatko, R. B. (2003) Metaphosphate in the active site of fructose-1,6-bisphosphatase, *J. Biol. Chem.* (in press).
39. Lahiri, S. D., Zhang, G., Dunaway-Mariano, D., and Allen, K. N. (2003) The pentacovalent phosphorus intermediate of a phosphoryl transfer reaction, *Science 299*, 2067−2071.
40. Waas, W. F., and Dalby, K. N. (2001) Purification of a model substrate for transcription factor phosphorylation by ERK2, *Protein Expression Purif. 23*, 191−197.
41. Adams, J. A., and Taylor, S. S. (1992) Energetic limits of phosphotransfer in the catalytic subunit of cAMP-dependent protein kinase as measured by viscosity experiments, *Biochemistry 31*, 8516−8522.
42. Cole, P. A., Burn, P., Takacs, B., and Walsh, C. T. (1994) Evaluation of the catalytic mechanism of recombinant human Csk (C-terminal Src kinase) using nucleotide analogs and viscosity effects, *J. Biol. Chem. 269*, 30880−30887.
43. Wang, C., Lee, T. R., Lawrence, D. S., and Adams, J. A. (1996) Rate-determining steps for tyrosine phosphorylation by the kinase domain of v-fps, *Biochemistry 35*, 1533−1539.
44. Chen, G., Porter, M. D., Bristol, J. R., Fitzgibbon, M. J., and Pazhanisamy, S. (2000) Kinetic mechanism of the p38-alpha MAP kinase: phosphoryl transfer to synthetic peptides, *Biochemistry 39*, 2079−2087.
45. Murray, B. W., Padrique, E. S., Pinko, C., and McTigue, M. A. (2001) Mechanistic effects of autophosphorylation on receptor tyrosine kinase catalysis: enzymatic characterization of Tie2 and phospho-Tie2, *Biochemistry 40*, 10243−10253.
46. Ablooglu, A. J., and Kohanski, R. A. (2001) Activation of the insulin receptor's kinase domain changes the rate-determining step of substrate phosphorylation, *Biochemistry 40*, 504−513.
47. Hagopian, J. C., Kirtley, M. P., Stevenson, L. M., Gergis, R. M., Russo, A. A., Pavletich, N. P., Parsons, S. M., and Lew, J. (2001) Kinetic basis for activation of CDK2/cyclin A by phosphorylation, *J. Biol. Chem. 276*, 275−280.
48. Simopoulos, T. T., and Jencks, W. P. (1994) Alkaline phosphatase is an almost perfect enzyme, *Biochemistry 33*, 10375−10380.
49. Grant, B. D., and Adams, J. A. (1996) Pre-steady-state kinetic analysis of cAMP-dependent protein kinase using rapid quench flow techniques, *Biochemistry 35*, 2022−2029.
50. Jan, A. Y., Johnson, E. F., Diamonti, A. J., Carraway, K. L., III, and Anderson, K. S. (2000) Insights into the HER-2 receptor tyrosine kinase mechanism and substrate specificity using a transient kinetic analysis, *Biochemistry 39*, 9786−9803.
51. Enke, D. A., Kaldis, P., and Solomon, M. J. (2000) Kinetic analysis of the cyclin-dependent kinase-activating kinase (Cak1p) from budding yeast, *J. Biol. Chem. 275*, 33267−33271.
52. Shaffer, J., Sun, G., and Adams, J. A. (2001) Nucleotide release and associated conformational changes regulate function in the COOH-terminal Src kinase, Csk, *Biochemistry 40*, 11149−11155.
53. Aubol, B. E., Nolen, B., Vu, D., Ghosh, G., and Adams, J. A. (2002) Mechanistic insights into Sky1p, a yeast homologue of the mammalian SR protein kinases, *Biochemistry 41*, 10002−10009.
54. Khokhlatchev, A. V., Canagarajah, B., Wilsbacher, J., Robinson, M., Atkinson, M., Goldsmith, E., and Cobb, M. H. (1998) Phosphorylation of the MAP kinase ERK2 promotes its homodimerization and nuclear translocation, *Cell 93*, 605−615.
55. Park, C., and Raines, R. T. (2003) Catalysis by ribonuclease a is limited by the rate of substrate association, *Biochemistry 42*, 3509−3518.
56. Zhang, F., Robbins, D. J., Cobb, M. H., and Goldsmith, E. J. (1993) Crystallization and preliminary X-ray studies of extracellular signal-regulated kinase-2/MAP kinase with an incorporated His-tag, *J. Mol. Biol. 233*, 550−552.
57. Pecoraro, V. L., Hermes, J. D., and Cleland, W. W. (1984) Stability constants of Mg^{2+} and Cd^{2+} complexes of adenine nucleotides and thionucleotides and rate constants for formation and dissociation of MgATP and MgADP, *Biochemistry 23*, 5262−5271.
58. Mansour, S. J., Candia, J. M., Matsuura, J. E., Manning, M. C., and Ahn, N. G. (1996) Interdependent domains controlling the enzymatic activity of mitogen-activated protein kinase kinase 1, *Biochemistry 35*, 15529−15536.
59. Bradford, M. M. (1976) A rapid and sensitive method for the quantitation of microgram quantities of protein utilizing the principle of protein-dye binding, *Anal. Biochem. 72*, 248−254.
60. Gill, S. C., and von Hippel, P. H. (1989) Calculation of protein extinction coefficients from amino acid sequence data, *Anal. Biochem. 182*, 319−326.
61. Linse, K. D., Smith, S., and Gadush, M. (1997) Development of a method for analysis of free amino acids from physiological samples using a 420A ABI/PE amino acid analyzer, in *Techniques in Protein Chemistry* (Marshak, D. R., Ed.) Vol. VIII, pp 197−205, Academic Press, San Diego.
62. Waas, W. F., Lo, H. H., and Dalby, K. N. (2001) The kinetic mechanism of the dual phosphorylation of the ATF2 transcription factor by p38 mitogen-activated protein (MAP) kinase alpha. Implications for signal/response profiles of MAP kinase pathways, *J. Biol. Chem. 276*, 5676−5684.
63. Canagarajah, B. J., Khokhlatchev, A., Cobb, M. H., and Goldsmith, E. J. (1997) Activation mechanism of the MAP kinase ERK2 by dual phosphorylation, *Cell 90*, 859−869.
64. Adachi, M., Fukuda, M., and Nishida, E. (1999) Two co-existing mechanisms for nuclear import of MAP kinase: passive diffusion of a monomer and active transport of a dimer, *EMBO J. 18*, 5347−5358.
65. Matsubayashi, Y., Fukuda, M., and Nishida, E. (2001) Evidence for existence of a nuclear pore complex-mediated, cytosol-independent pathway of nuclear translocation of ERK MAP kinase in permeabilized cells, *J. Biol. Chem. 276*, 41755−41760.
66. Whitehurst, A. W., Wilsbacher, J. L., You, Y., Luby-Phelps, K., Moore, M. S., and Cobb, M. H. (2002) ERK2 enters the nucleus by a carrier-independent mechanism, *Proc. Natl. Acad. Sci. U.S.A. 99*, 7496−7501.
67. Shaffer, J., and Adams, J. A. (1999) Detection of conformational changes along the kinetic pathway of protein kinase A using a catalytic trapping technique, *Biochemistry 38*, 12072−12079.

APPENDIX

Herein, we present observations that the catalytic constant k_{cat} for ERK2 varies with ERK2 concentration. These data are discussed in the context of published biochemical evidence for ERK2 dimerization, and a kinetic model is presented.

Sensitivity of the Catalytic Constant to the Concentration of ERK2. The k_{cat} value of 37 s^{-1} determined under pre-steady state conditions is significantly higher than values routinely determined under steady state conditions. To determine whether the difference is due to the higher concentrations of ERK2 used in the pre-steady state experiments, k_{cat} was measured over a range of ERK2 concentrations.

In these experiments, ERK2 (4−8400 nM) was preincubated with a saturating concentration of EtsΔ138 (400 μM), in buffer A3 containing 20 mM $MgCl_2$, before rapid mixing with an equal volume of $MgATP^{2-}$ (8 mM) in the same buffer (20 mM total Mg^{2+}). After 2−150 ms, reactions were quenched with acid. The catalytic constant, k_{cat}, was determined from the slope of the linear portion of a plot of [EDP] + [P] versus time, according to the relationship $k_{cat} = v_{ss}/[E_0]$. Figure 5 shows that the observed magnitude of k_{cat} increases as the concentration of ERK2 increases from 2 to 4200 nM. This dependence is consistent with the formation of higher-order complexes of ERK2 as the concentration increases. As there is only a small difference in the specific activity of ERK2 at low and high concentrations, defining a trend is difficult given the errors associated with the rapid quench technique.

Scheme 2

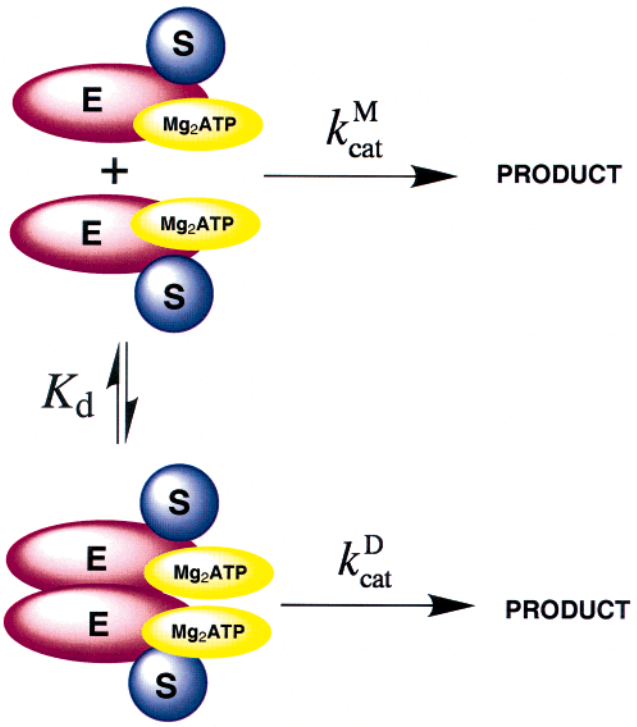

There is, however, some evidence that ERK2 forms activated homodimers. For example, equilibrium sedimentation analysis suggested that a homodimer dissociates with a dissociation constant K_d of 7.5 nM at 4 °C (*1*). Interestingly, homodimerization appears to be an integral part of MAPK cell signaling and perhaps serves to regulate its nuclear transport (*2*−*4*). For example, it has been proposed that dimerization of active ERK2 is required for its active nuclear transport (*2*−*4*), an event that is profoundly important for ERK2 signaling (*5*−*7*).

The structural basis for the formation of a possible homodimer was revealed through X-ray crystallography (*8*). Khokhlatchev *et al*. suggested that two loops on ERK2, termed the activation loop and the C-terminal extension loop (loop 16), are responsible for the tight interaction of the dimer. The fact that both of these loops also appear to play a role in ERK2 activation provides a potential link between the oligomerization state of the enzyme and its activity (*1*, *8*). While it should be noted that an N-terminal His_6 tag has previously been shown to promote the dimerization of a protein (*9*), it is unlikely to be the case for ERK2, because the His_6 tag does not comprise part of the dimerization interface identified in the crystal structure (*8*). Thus, the available evidence suggests that ERK2 forms a dimer once activated, and the data presented here are consistent with the notion that dimerization moderately influences its activity.

Kinetic Model of Dimerization. Equation A1 describes the kinetic dependence on ERK2 dimerization according to Scheme 2 where the monomeric and dimeric forms of ERK2 have specific activities (per active site) of k_{cat}^M and k_{cat}^D, respectively. Limiting values for k_{cat}^M and k_{cat}^D were estimated from studies at low and high concentrations of ERK2. Using a k_{cat}^M value of 25 s^{-1} and a k_{cat}^D value of 37 s^{-1}, the best fit to the data, according to eq A1 (see below), provides an estimate for the dissociation constant for the dimer, K_d, of 32 ± 16 nM. This is similar to the value reported by Khokhlatchev *et al*. (*1*).

While the data in Figure 5 are not of sufficient quality to critically define this model, it does lend credence to the notion that ERK2 forms a dimer in the low nanomolar range. The homodimerization model, in which ERK2 monomers and dimers differ in activity, assumes that the monomers retain their activity in the dimeric form. According to this model, either k_2, k_3, or both are modulated slightly upon dimerization which results in a slight increase in k_{cat}. This could explain why Prowse *et al*. failed to see rate-limiting product release when studying ERK2 at low concentrations (*10*).

Derivation of Equation A1. The equation describing the dependence of k_{cat} on the concentration of ERK2 according to the dimerization in Scheme 2 is derived as follows.

At a given concentration of ERK2, E_0, the observed maximal velocity, V_{max}^{obs}, is given by

$$V_{max}^{obs} = k_{cat}^{obs}E_0 = k_{cat}^{M}E_M + 2k_{cat}^{D}E_D \quad \text{(i)}$$

where E_M and E_D are the concentrations of complexes containing monomeric and dimeric ERK2, respectively.

Conservation of mass then gives

$$E_0 = E_M + 2E_D \quad \text{(ii)}$$

where E_0 is the concentrations of total enzyme.

Substitution of eq ii into eq i gives

$$k_{cat}^{obs}E_0 = k_{cat}^{M}(E_0 - 2E_D) + k_{cat}^{D}E_D \quad \text{(iii)}$$

The dissociation constant of the complex in Scheme 2 is given by

$$K_d = (E_M E_M)/E_D \quad \text{(iv)}$$

Substitution of eq ii into eq iv gives

$$K_d = (E_0 - 2E_D)^2/E_D \quad \text{(v)}$$

Using eq iii and the real solution to eq v, the observed catalytic constant k_{cat}^{obs} is given by

$k_{cat}^{obs} = k_{cat}^{M}(E_0 - 2E_D) + k_{cat}^{D}E_D/E_0$, where

$$E_D = \frac{4E_0 + K_d - \sqrt{K_d^2 + 8K_dE_0}}{8} \quad \text{(A1)}$$

APPENDIX REFERENCES

1. Khokhlatchev, A. V., Canagarajah, B., Wilsbacher, J., Robinson, M., Atkinson, M., Goldsmith, E., and Cobb, M. H. (1998) Phosphorylation of the MAP kinase ERK2 promotes its homodimerization and nuclear translocation, *Cell 93*, 605−615.
2. Adachi, M., Fukuda, M., and Nishida, E. (1999) Two co-existing mechanisms for nuclear import of MAP kinase: passive diffusion of a monomer and active transport of a dimer, *EMBO J. 18*, 5347−5358.
3. Matsubayashi, Y., Fukuda, M., and Nishida, E. (2001) Evidence for existence of a nuclear pore complex-mediated, cytosol-independent pathway of nuclear translocation of ERK MAP kinase in permeabilized cells, *J. Biol. Chem. 276*, 41755−41760.
4. Whitehurst, A. W., Wilsbacher, J. L., You, Y., Luby-Phelps, K., Moore, M. S., and Cobb, M. H. (2002) ERK2 enters the nucleus

by a carrier-independent mechanism, *Proc. Natl. Acad. Sci. U.S.A. 99*, 7496−7501.
5. Pouyssegur, J., Volmat, V., and Lenormand, P. (2002) Fidelity and spatio-temporal control in MAP kinase (ERKs) signalling, *Biochem. Pharmacol. 64*, 755−763.
6. Volmat, V., and Pouyssegur, J. (2001) Spatiotemporal regulation of the p42/p44 MAPK pathway, *Biol. Cell 93*, 71−79.
7. Volmat, V., Camps, M., Arkinstall, S., Pouyssegur, J., and Lenormand, P. (2001) The nucleus, a site for signal termination by sequestration and inactivation of p42/p44 MAP kinases, *J. Cell Sci. 114*, 3433−3443.
8. Canagarajah B. J., Khokhlatchev, A., Cobb, M. H., and Goldsmith, E. J. (1997) Activation mechanism of the MAP kinase ERK2 by dual phosphorylation, *Cell 90*, 859−869.
9. Wu, J., and Filutowicz, M. (1999) Hexahistidine (His_6)-tag dependent protein dimerization: a cautionary tale, *Acta Biochim. Pol. 46*, 591−599.
10. Prowse, C. N., Hagopian, J. C., Cobb, M. H., Ahn, N. G., and Lew, J. (2000) Catalytic reaction pathway for the mitogen-activated protein kinase ERK2, *Biochemistry 39*, 6258−6266.

BI0348617